# Performance Evaluation of Circuit Breaker Electrical Contact Based on Dynamic Resistance Signature and Using Health Index

Maryam Khoddam, Javad Sadeh, and Pedjman Pourmohamadiyan

***Abstract*— High-voltage circuit breakers (CBs) are extremely important components for the function of power supply system. The need to predict proper function of CB has increased over the years. Dynamic resistance measurement (DRM) is an effective method to evaluate the condition of CB's contact. This paper aims to predict the correlation between the various levels of contact degradation and characteristics of dynamic resistance waveform. Five diagnosis parameters are extracted from DRM curve. Using scoring and weighting techniques, heath index is applied to clearly identify the condition of CB as healthy, need caution, and risky. The proposed method is implemented with ten healthy and ten faulty electrical contacts as examples for illustrating the effectiveness of the method in assessing the CB condition.**

***Index Terms*— Condition assessment, dynamic resistance measurement (DRM), electrical contact, health index (HI).**

## I. Introduction

CIRCUIT breakers (CBs) are vital components at substation for power system reliability and protection [1], [2]. The monitoring of CBs has been recognized as beneficial due to their critical role in the power system operation.

A CB is expected to reliably perform trip and close operation during its service life. The design of modern high-voltage puffer-type $SF_6$ gas CBs is based on the switching of two parallel contact sets. First, the main contacts are designed to carry the load current without any excessive temperature rise, and thus they do not degrade by the effects of the arcing. Second, the arcing contacts operate at breaker opening following the main contacts' part. The arc, which is formed after the separation of the arcing contacts, is cleared at the next current zero crossing [3]. The arcing contacts conduct the arcing current, and therefore are submitted to the arcing discharge and all of its effects during the fault opening operation [4]–[6]. The energy released by the electric arcing has the ability to induce rapid material erosion at the arcing contacts.

This erosion and thus the change in contact geometry directly reflect on a significant decrease in the breaking capacity and working condition of the CB and associated electrical circuit [5]–[9].

To assess the condition of breaker contacts, the main contact resistance measurement is usually performed. This measurement does not give any indication of the condition of the arcing contacts [4]. To evaluate the arcing contact condition, an internal inspection can be done. Disassembly of breakers that have no defects means unnecessary expenses and may also lead to, or accelerate, the onset of new problems in the equipment [5]. A useful parameter to effectively diagnose the electrical contact failures is dynamic resistance measurement (DRM). This method is performed when the breaker is out of service and consists of applying high dc current through the contact system, measuring the voltage drop across the contact and calculating the resistance. The DRM has been investigated from various perspectives in the literature. For instance, [4] reports effects of metallic products produced during arc quenching on contact resistance in $SF_6$ CB. Landry *et al.* [6] suggest that the DRM test should carry out at low speed (0.002–0.2 m/s) in the case of reproducible resistance curve to be obtained, but Šečić and Milovic [10] report that this method is instructive for some breaker mechanisms. Since an adjustment to the operating mechanism is required, there is a potential risk of damaging the operating mechanism when restoring it back in service. In [11]–[13], several spikes in the resistance curves are depicted, which could be the result of a partial contact part during the contact separation. Reference [14] describes the use of Arduino platform as a solution for measuring the dynamic contact resistance curve. This platform is an open-source electronic prototyping platform that can receive analog or digital input from a variety of sensors. However, it has some limitations such as the sampling rate. Reference [15] proposes a software solution for analyzing the dynamic resistance measurement results for high-voltage CB. This software is capable of calculating the static resistance, overlapping time, and distance using dynamic resistance and motion waveforms instantly. However, this software does not reveal the normal/abnormal status of

Manuscript received February 24, 2016; revised June 4, 2016; accepted July 31, 2016. Date of publication September 14, 2016; date of current version October 13, 2016. Recommended for publication by Associate Editor J. McBride upon evaluation of reviewers' comments.

The authors are with the Electrical Engineering Department, Faculty of Engineering, Ferdowsi University of Mashhad, Mashhad 9177948974, Iran (e-mail: marya.khoddam@stu.um.ac.ir; sadeh@um.ac.ir; pourmohamadiyan@um.ac.ir).

Color versions of one or more of the figures in this paper are available online at http://ieeexplore.ieee.org.

Digital Object Identifier 10.1109/TCPMT.2016.2601316

2156-3950 © 2016 IEEE. Personal use is permitted, but republication/redistribution requires IEEE permission.
See http://www.ieee.org/publications_standards/publications/rights/index.html for more information.

Authorized licensed use limited to: Electricity Generating Authority of Thailand. Downloaded on January 15,2021 at 00:33:40 UTC from IEEE Xplore. Restrictions apply.

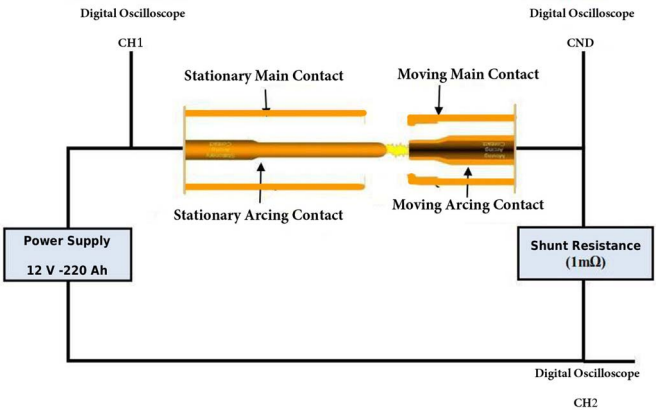



Fig. 1. Experimental setup.

the contacts and interpretation of the results still depends on operator knowledge. DRM parameters that can assist in the contacts diagnosis are introduced in [6] and [16]. According to their results, the evolution of the curve area is directly proportional to the wear level of the main and arcing contacts. More research should be carried out to consider other contact defects to assure curve area as a signature for contact wear.

Moreover, none of the works carried out till now contributed to the comprehensive investigations which correlate the data extracted from dynamic resistance curve to the level of contact failure. This paper aims to evaluate a relationship between various levels of degradation of the contacts and change in dynamic resistance parameters. Through application of data mining on dynamic resistance curve and using health index (HI), a condition assessment process is proposed. This is to prepare a decision-making strategy for distinguishing normal versus faulty condition.

In order to study damage extent of electrical contact on dynamic resistance curve and to survey the possibility of contact failure in operation, measurements are gathered from four similar samples of fixed and mobile electrical contacts. One of these contacts is in good condition, while the other three contacts are exposed to intentional malfunctions, i.e., contact misalignment, erosion of arcing contact, and damage due to welding of contact material. To obtain a greater accuracy in the level of contact degradation and DRM curve, monitoring of the process since the initial stage until advanced stages of defect is suggested.

Having delved into recorded data, five diagnosis features are extracted. Scoring and weighting techniques are applied for performance evaluation. The results are indicated in terms of the performance index of electrical contact. Therefore, an appropriate maintenance schedule can be reasonably planned.

## II. Experimental System

Dynamic contact resistance measurement is an effective method to represent the actual condition of main and arcing contacts without dismantling the CB. The experimental apparatus is designed to controllably open a pair of contacts. DRM is measured during close–open operation. Fig. 1 shows a schematic of the break apparatus and arrangement of the additional facilities.

The test current is delivered by a regular 12 V/220-Ah car battery. The minimum dc test current should be 100 A, and the use of higher current value provides a reliable voltage drop reading, thus allowing exact detection of the contacts' performance [17]. The current passing the contacts is measured via a 1-mΩ noninductive shunt resistance. All signals are recorded with a digital storage oscilloscope with 50-GHz bandwidth. The contacts open at a constant velocity of 0.2 m/s, controlled by the opening control mechanism to keep the system variables to a minimum. In this way, resistance curves are smoother and reproducible from one test to another. Moreover, main contact part can be easily identified at low contact speed [5]. By injecting a high current through the contacts, simultaneously monitoring the voltage drop across the main contact during the opening operation, and by dividing instantaneous voltage to current, DRM curve will be acquired [4]. The DRM results are usually presented in contact resistance (Ω) versus displacement of moving contact (mm) or time of operation (s) [15].

During each opening operation, depending on the rms value of the switched current, a fraction of the arcing contact material burns away. This leads to a shorter time difference—between the separation of the nominal contacts and the separation of the arcing contacts—during the next switching operation. This time difference is called the contact overlap time. The electrical contact requires overhaul when the contact overlap time has fallen below a defined minimum value. Any further operation may cause the interrupting chamber to explode [18].

## III. Working Procedure

In order to scrutinize the impact of different failures on DRM waveforms, measurements are gathered from four similar electrical contacts. One of these contacts is in good condition, while three other contacts are exposed to intentional malfunctions as follows.

1) *Erosion of Arcing Contact:* Arcing in high-voltage CB leads to material erosion at the arcing contact. It is known that the erosion of contact material depends on some parameters like the arcing current amplitude, arcing time, total charge, and contact material properties. The amount of eroded arcing contact is a main factor that determines the end of the lifetime of a CB [6].
2) *Contact Misalignment:* Due to misalignment of arcing contact at the break assembly, damage to fixed arcing contact can happen. This condition changes the contact geometry as well and yields to imperfect performance of CB.
3) *Deformation Caused by Welding of Contact Material:* It has long been known that the process of melting and boiling of contact material occurs due to heating caused by energy fluxes on the arcing contact deduced from the high-temperature arc plasma. Appearance of spot welds on contact area will accelerate the contact erosion.

In all these cases, there is an increased risk for excess heat within the CB, with the possibility of reaching higher temperatures than the CB is designed for, and thereby the probability of explosion of the breaker [4].

Authorized licensed use limited to: Electricity Generating Authority of Thailand. Downloaded on January 15,2021 at 00:33:40 UTC from IEEE Xplore. Restrictions apply.

TABLE I
DESCRIPTION OF DYNAMIC RESISTANCE FEATURES

| Feature | Description |
|---|---|
| $R_a$ (mΩ) | Average arcing contact resistance before the beginning of vertical slope of DRM curve |
| $R_p$ (mΩ) | Average main contact resistance |
| $R_a.T_a$ (mΩ.ms) | Cumulative area beneath the dynamic contact resistance curve just before the maximum value reached just before the arcing contact part |
| $T_{ov}$ (ms) | Time difference between separation of the main and arcing contact |
| $R_{a,max}$ (mΩ) | Maximum value of resistance just before the arcing contact part |

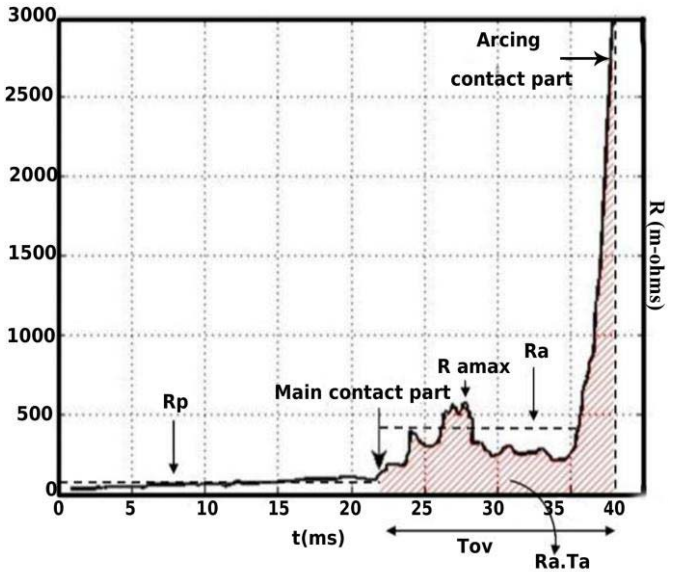



Fig. 2. Typical DRM curve with suggested diagnosis parameters.

To obtain a greater accuracy in diagnosing the level of contact degradation and DRM curve, monitoring of the process since the initial stage until advanced stages of defect is suggested.

### *A. Effective Diagnosis Features Extracted From Dynamic Resistance Measurement*

DRM is used as a diagnostic method to identify CBs' electrical contacts' abnormalities. Any defects on the contact structure will affect the resistance value of the main and/or arcing contact. However, it should be noted that low levels of resistance do not mean the chamber is in good condition [3]. In order to ensure the condition of contacts, some other diagnosis features must be defined and used. These features should provide comprehensive and effective insight into the condition of component. Table I presents five diagnosis parameters reflecting the electrical contact abnormalities. Fig. 2 depicts a typical DRM curve and diagnosis parameters.

An increase or decrease in the above-mentioned features can be used to discriminate between the healthy and the faulty electrical contacts. Although the ranges of selected features are depended on the electrical contact characteristics, e.g., contact shape and contact material, the changes in their values will reveal some abnormalities in electrical contact regardless of contact properties.

The efficiency of these parameters in condition assessment of CB has been proved through experimental tests.

TABLE II
RANGE, MEAN, AND STANDARD DEVIATION OF SELECTED FEATURES DURING NORMAL CONDITION

| Features | Range | Mean | Standard Deviation |
|---|---|---|---|
| $R_a$ (mΩ) | 2.86-3.235 | 3.027 | 0.0615 |
| $R_p$(mΩ) | 0.52-1.21 | 0.7113 | 0.1749 |
| $R_a$.Ta ((mΩ.ms) | 351.1-1648.1 | 876.8 | 262.2 |
| $T_{ov}$ (ms) | 11.72-15.01 | 12.32 | 0.1906 |
| $R_{a,max}$ | 4.2328-5.092 | 4.612 | 0.081 |

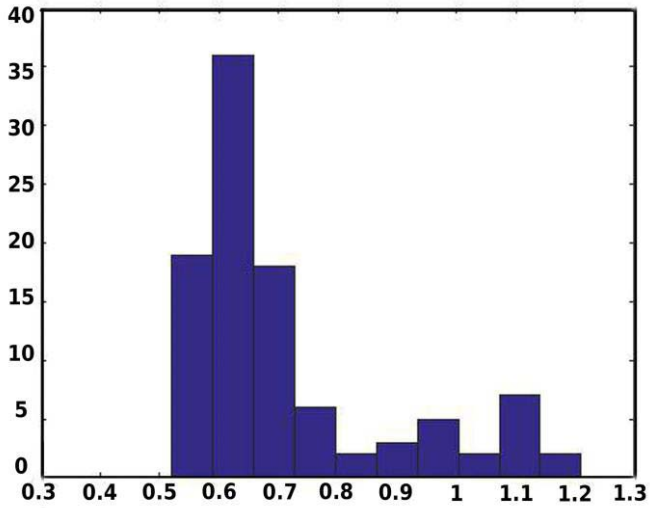


Fig. 3. Frequency distribution related to $R_p$ during 100 normal tests.

### *B. Normal Values of Selected Features*

To inquire the impact of damage extent on dynamic resistance curve, it is necessary to determine the normal value of selected features of DRM. The characteristic parameters of DRM have a statistical nature, so a large number of measurements are to be done. For this purpose, DRM is carried out 100 times during normal operation, and then features' range, mean, and standard deviation are calculated. The results are summarized in Table II.

Fig. 3 represents the frequency distribution of the recorded data for $R_p$ during 100 normal condition tests. The mean value of this feature is about 0.71 mΩ, and its standard deviation is about 0.18 mΩ. Referring to Table II, it can be concluded that if their changes due to the failure are much larger than their statistical variation, then these may be used for electrical contact failure detection.

Fig. 4 shows the frequency distribution of the recorded data for $R_p$ during 100 faulty operation tests. The value of $R_p$ during faulty condition differs from 0.58 to 2.96 mΩ, while its mean gets a value of 0.9511 mΩ. Thus, one can deduce that low value of $R_p$ does not guarantee good condition of chamber.

Authorized licensed use limited to: Electricity Generating Authority of Thailand. Downloaded on January 15,2021 at 00:33:40 UTC from IEEE Xplore. Restrictions apply.

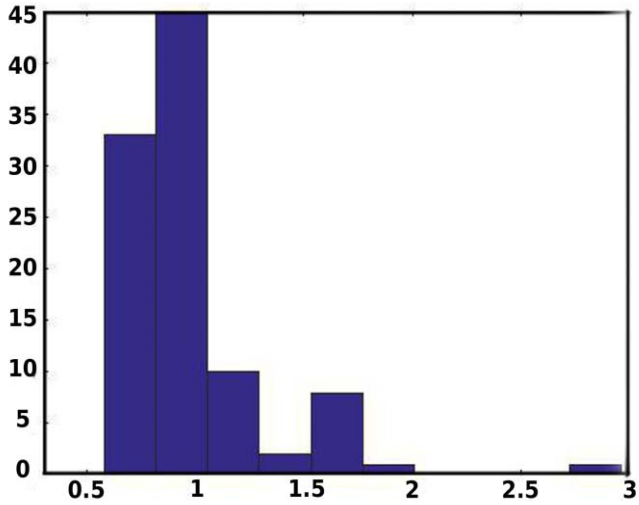



Fig. 4. Frequency distribution related to $R_p$ during 100 faulty tests.

TABLE III
SCORING OF EACH FEATURE BASED ON FAILURE RATE

| Feature type | Score | | |
|---|---|---|---|
| | 1 (Low) | 3 (Medium) | 5 (High) |
| Type I | $< \mu-\sigma$ | $\geq \mu-\sigma$ & $< \mu+\sigma$ | $\geq \mu+\sigma$ |
| Type II | $\geq \mu+\sigma$ | $\geq \mu-\sigma$ & $< \mu+\sigma$ | $< \mu-\sigma$ |

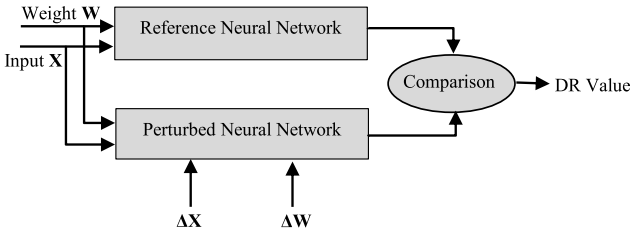



Fig. 5. General structure for investigating the effects of perturbation [26].

### C. Scoring and Weighting Techniques

The scoring and weighting techniques are in the form of multicriterion analysis. In this paper, they are used for classifying the condition of CB electrical contact into three levels: healthy, need caution, and risk. It involves identification of the nonmonetary factors that are relevant to the project. The relative importance of each criterion is determined by allocating of weights, while the allocation of scores to each option reflects how it performs in relation to each attribute [18]. The scoring of features is classified into three levels depending on failure rate. The failure rate gives the estimated probability that a device or component will fail during a full year of use. When a device failure probability exceeds a certain value, an intervention is suggested.

In this paper, the level of failure rate is specified by the use of mean ($\mu$) and standard deviation ($\sigma$) as explained in the following.

For indices of type I, which the smaller value indicates better condition, for example, $R_p$, the relative impairment grade index is calculated as follows.

Each feature that has failure rate lower than one standard deviation from its mean has a score of one as given in low failure rate group. Features with failure rate greater than one standard deviation plus the mean have a score of five, and features between these two groups have a score of three.

For an index in which the larger value is preferred (type II), i.e., $T_{\text{ov}}$, the relative importance is computed in the following approach.

If the feature's failure rate is less than one standard deviation from its mean, then it will have a score of five, while features with failure rate more than one standard deviation plus the mean will have a score of one, and features between these two groups have a score of three.

The results are summarized in Table III.

To assess the overall condition of an equipment, it is necessary to include as much data as available and to determine the relative degree of importance of the different condition factors in detecting the health of the asset. Many decision making methods such as analytical hierarchy process, fuzzy logic, gray theory, and evidence theory have been used to tackle uncertainty [20]–[23]. In these approaches, the weights and indices are determined based on experts' interviews and feedbacks. However, in the CB's electrical contacts' condition assessment process through DRM curve, these data are not precisely determined and available. In this paper, the weighting factors are determined through sensitivity analysis. Several methods such as differential approach, Monte Carlo analysis, response surface methodology, and Fourier amplitude sensitivity test have been developed to perform sensitivity studies. These approaches are based on Taylor series expansion, random sampling, response surface construction, and Fourier series, respectively [24]. In this paper, we focus on differential approach. Differential approach is based on using Taylor series. This method describes the relationship between the perturbed response of the function and parameter perturbation. For example, for 1-D cost function $f$, the Taylor expansion is written as follows:

$$f(\theta+\Delta\theta) = f(\theta) + \frac{\Delta\theta}{1!}f'(\theta) + \frac{\Delta\theta^2}{2!}f''(\theta) + \cdots \quad (1)$$

where $\theta$ is a parameter and $\Delta\theta$ is a small perturbation of $\theta$.

An easy way to do sensitivity analysis based on differential approach is using artificial neural networks. These networks are reliable algorithms to perform functional input/output mapping. This mapping is generated for different input conditions, and then can be easily exploited in an uncertainly analysis. Moreover, the network can provide an indication of the importance of the various inputs in terms of the effects of variation in their values on the output (first-order sensitivity coefficient) [25]. Sensitivity refers to how a neural network output is influenced by its input and/or weights perturbations. For the purpose of analysis, these perturbations can be simulated by embedding disturbance to the original inputs or connection weights [26]. Fig. 5 shows how to investigate the effects of small perturbations to neural networks.

A small change in input may change the neural network's output result. Inspection of the mean square error allows

Authorized licensed use limited to: Electricity Generating Authority of Thailand. Downloaded on January 15,2021 at 00:33:40 UTC from IEEE Xplore. Restrictions apply.

TABLE IV
VALUE OF DECISION ERROR OF SELECTED FEATURES

| | $R_{a,max}$ | $R_a$ | $R_a.T_a$ | $T_{ov}$ | $R_P$ |
|---|---|---|---|---|---|
| DR | 0.2438 | 0.135 | 0.098 | 0.096 | 0.052 |

TABLE V
VALUE OF DECISION ERROR OBTAINED BY SECOND-ORDER UNCERTAINTY ANALYSIS

| Combined features | DR | Combined features | DR |
|---|---|---|---|
| $R_{a,max}$ , $R_a$ | 1.6757 | $R_a$ , $R_a.T_a$ | 0.6179 |
| $R_{a,max}$ , $R_a.T_a$ | 1.2318 | $R_a$ , $T_{ov}$ | 0.7144 |
| $R_{a,max}$ , $T_{ov}$ | 1.3691 | $R_a.T_a$ , $T_{ov}$ | 0.603 |
| $R_{a,max}$ , $R_p$ | 0.5749 | $R_a.T_a$ , $R_p$ | 0.144 |
| $R_a$ , $R_p$ | 0.0473 | $T_{ov}$ , $R_p$ | 0.151 |

determining which input affects the output most. The response of the network to weight and input errors is called decision error (DR), which is defined as the absolute difference between the decision made by the reference system and that made by the perturbed system. A small value of $DR_i$ in comparison to others means that the $i$th input does not significantly contribute to output.

Using this technique, Gaussian noise with a signal-to-noise ratio of ten is added to just one input, whereas other inputs are left unaltered (first-order uncertainty analysis). Then, DR related to that input is calculated. The results are shown in Table IV. We can proceed further and consider also the combination of the two inputs by varying both quantities simultaneously (second-order uncertainty analysis).

Table V provides the results obtained by the second-order uncertainty analysis.

Based on DR values in Tables IV and V, it can be concluded that $R_{a,max}$ is the most important input, and a small change in its value causes the output results to face a large error, while according to the DR value of $R_p$, this input has the less effect on the output results. The reason lies in fact that most defects are created on arcing contact where energy fluxes from the arc are imposed. Moreover, in some cases, the arcing contact peak reveals some abnormalities in the arcing contact, while the average value could be interrupted as normal condition. Thus, it is reasonable that $R_{a,max}$ gets a larger weight in comparison to $R_a$. Overlap time is also affected by arcing characteristics, but main contacts that carry the load current do not damage because of arc energy fluxes. Therefore, it is reasonable that $R_p$ is assigned with the least weight among five diagnosis factors.

In accordance with DR values and pairwise comparison, weighting factors of selected parameters are extracted. Table VI indicates the parameter's final weights.

TABLE VI
WEIGHTING FACTORS OF FIVE FEATURES

| **Feature** | **Weight** |
|---|---|
| $R_{a,max}$ | 10 |
| $R_a$ (mΩ) | 6 |
| $R_a.T_a$ (mΩ.ms) | 3 |
| $T_{ov}$ | 3 |
| $R_p$ (mΩ) | 1 |

## IV. PERFORMANCE EVALUATION USING HEALTH INDEX

In POWERGRID, there have been failures of breakers due to damages in components in the interrupting chambers much before ten years. Defects were noted in the components of few CBs before completion of ten years, whereas few CBs that were 17–20 years in service were healthy [27], [28]. This is where the time base maintenance drawback is evident. Condition-based maintenance (CBM) monitors the operation condition of the power equipment in real time to calculate and analyze the trends of the changes and to decide if maintenance activity is needed [20]. For diagnostic testing to decide for overhauling, HI can be used [29], [30]. Condition of an asset will be accurately revealed, if HI includes as much data as is available and suitable for realistic assessment. In the case of electrical contacts, based on DRM selected features and scoring-weighting techniques, the renovation index (RI%) and HI% are calculated as given in (2) and (3), respectively [29]. Using HI index, the condition of CB's electrical contact classifies into three levels as healthy, need caution, and risk. It should be noted that high RI refers to the high requirement of equipment renovation and the higher HI reveals the better condition

$$\mathrm{RI}\% = \frac{\sum_{i=1}^{n} s_i \times w_i}{s_{i,\max} \sum_{i=1}^{n} w_i} \tag{2}$$

$$\mathrm{HI}\% = 100 - \mathrm{RI}\% \tag{3}$$

where $s_i$ and $w_i$ are the assigned score and weight to the $i$th feature, respectively.

The asset health scaling categories would correspond to probability of failure rates of an asset in its mechanical life [29], [31].

Mechanical life refers to the number of mechanical operations that can be expected from a CB, and it is a function of the current and voltage rating of the CB [32], where an HI% of 100 represents excellent condition and less than 25% represents very poor health condition. Table VII provides a summary of the condition assessment based on HI calculation. If HI% is above 85%, the electrical contact condition is categorized in healthy state. As mentioned above, there are some minor and serious deteriorations in good and fair operation, and thus for HI% between 50% and 85%, the contact operation needs caution, and preventive maintenance (PM) is suggested. Because there are major defects in operation with HI% below 50%, the contact operation will be risky. In this stage, corrective maintenance is the only reasonable choice. Fig. 6 shows the flowchart of the electrical contact condition assessment.

## V. RESULTS AND DISCUSSION

In order to scrutinize the level of defect on DRM curves, four pairs of contacts (samples A-D) are used. Each sample consists of a fixed contact and a mobile contact. Sample A is in fully healthy condition, while samples B-D are exposed to

Authorized licensed use limited to: Electricity Generating Authority of Thailand. Downloaded on January 15,2021 at 00:33:40 UTC from IEEE Xplore. Restrictions apply.

TABLE VII
HI SCALE

| Health Index (HI%) | Condition | Probability of failure (PF) | Description | Necessary action |
|---|---|---|---|---|
| 85-100 | Very good | Low | Some aging or minor deterioration | Normal maintenance |
| 70-85 | Good | Low but slightly increasing | Significant deterioration | Preventive maintenance |
| 50-70 | Fair | Rapidly increasing but lower than PF at mean mechanical life | Serious deterioration | Preventive maintenance |
| 25-50 | Poor | Increasing and higher than PF at mean mechanical life | Widespread significant deterioration | Corrective maintenance |
| 0-25 | Very poor | Very high, more than double the PF at mean mechanical life | Extensive significant deterioration and major failure | Corrective maintenance |

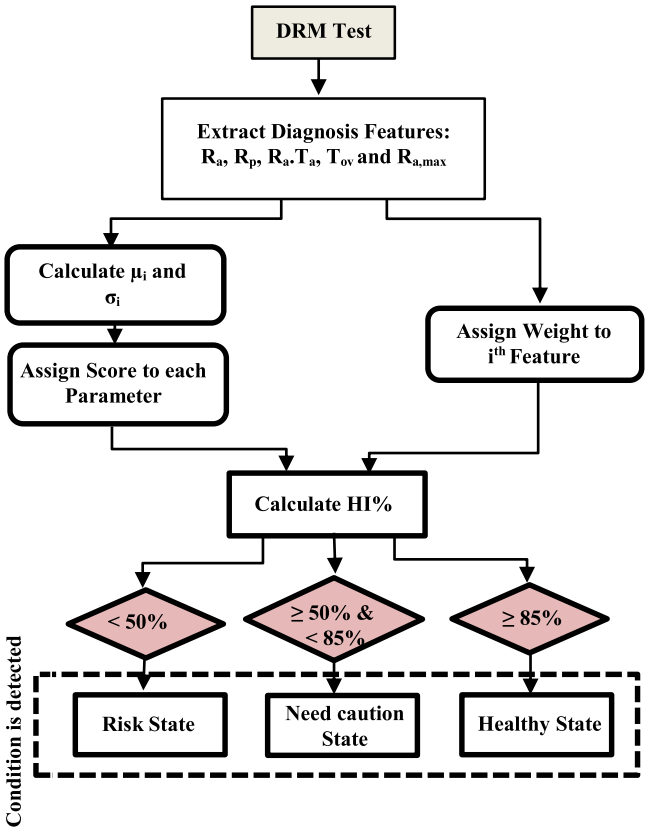



Fig. 6. Flowchart of the proposed diagnosis approach.

five accelerated degradation processes (erosion, misalignment, and deformation).

Considering statistical nature of selected features, for samples B-D, DRM is performed after each of the five degradation processes and repeated five times. Thus, there are 75 DRM curves gathered from samples B-D. Twenty-five consecutive resistance measurements are also done for the healthy contact.

Hence, through 100 tests during faulty and healthy condition, mean ($\mu$) and standard deviation ($\sigma$) of selected features are determined. As explained in Section III, scores of selected parameters are determined. Features with a score of five are classified in high failure rate group.

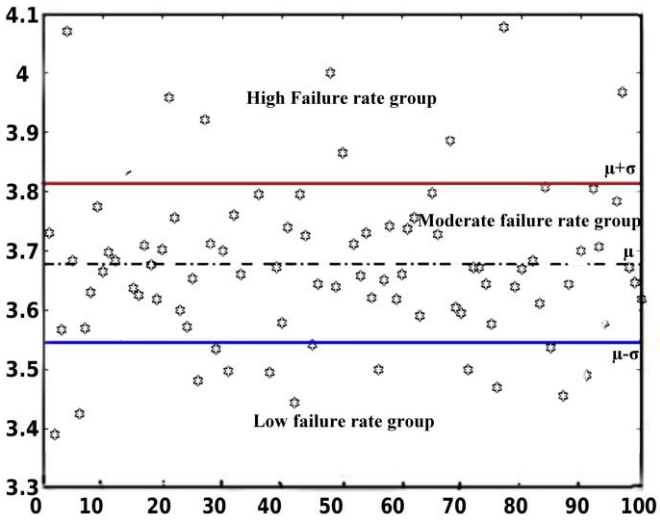



Fig. 7. Healthy, moderate, and risky zones for feature $R_a$.

Features with a score of three are categorized in moderate failure rate group, while features with a score of one are placed in low failure rate group. Fig. 7 shows three defined zones for feature $R_a$ during 100 tests.

Among 15 points that are classified in low failure rate group, 13 points are related to healthy contact, one point is connected to contact with misalignment, and one other point is related to contact with erosion defect. There are 74 points that are categorized as moderate failure rate, among them 12 points are related to healthy contacts and 23, 20, and 19 points are connected to misalignment, spot weld, and erosion defects, respectively. In high failure rate group, there are 11 points: one for misalignment, five for spot weld, and five for erosion failures. The results of this zone are related to severe damage on arcing contact area.

To illustrate the efficiency of the proposed method in condition assessment of electrical contact, DRM test is carried out for another group of ten healthy contacts and a group of ten faulty contacts. Defected contacts are selected randomly from three original faulty contact groups (B-D) as introduced before. Having scoring values of each criterion and its associated weight, the HI for these two groups is calculated. Fig. 8 shows

Authorized licensed use limited to: Electricity Generating Authority of Thailand. Downloaded on January 15,2021 at 00:33:40 UTC from IEEE Xplore. Restrictions apply.

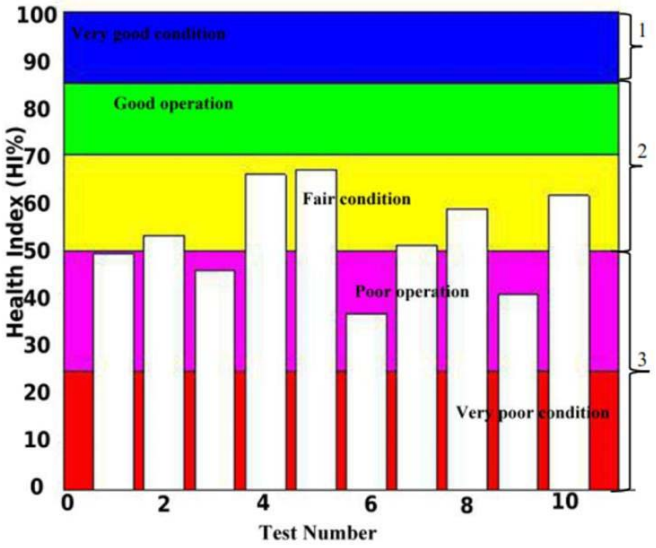



Fig. 8. Overall performance of ten faulty electrical contacts. 1: Healthy operation. 2: Need caution condition. 3: Risky operation.

the overall performance of ten faulty CB's electrical contact. There are four electric contacts in poor zone with risky condition. Other six electrical contacts are in fair zone, which means that their operation needs caution.

Calculating the HI%, the contact's looking condition is investigated, for example, checking four contacts in poor condition shows the following.

1) Contact number 1 with HI% = 49.45% is highly deformed caused by welding of the contact material.
2) Contact number 3 with HI% = 45.8% is also damaged in the arcing contact part, where the presence of spot welds is obvious.
3) Contact number 6 has an HI% of 37.05%. This contact was exposed with arcing contact misalignment, which also causes damage to the main contact part.
4) Effects of erosion of contact material are seen on contact number 9. HI% for this contact set is about 41%.

Other six contacts that are classified in fair condition mode have the following defects.

1) Contact numbers 2 and 8 are exposed to misalignment defect.
2) Contact numbers 4, 7, and 10 are damaged due to erosion.
3) Contact number 5 is defected in the arcing contact part because of the presence of some spot welds on it.

The poor performance is associated with high failure rate. Thus, those contacts should be planned for intensive inspection in order to reduce the failure rate and to improve the whole electrical system reliability. Table VIII presents the HI% for ten healthy electrical contacts. The results well indicate that all of ten contacts are categorized in very good and good condition classes.

In contacts that are categorized in good condition, some minor defects such as tiny spot welds were observed.

According to the results, the efficiency of suggested method for evaluating the condition of electrical contacts is realized.

TABLE VIII
HI% FOR TEN HEALTHY ELECTRICAL CONTACTS

| Test Number | HI% | Condition |
|---|---|---|
| (1) | 87.60 | Very Good |
| (2) | 83.00 | Good |
| (3) | 90.23 | Very Good |
| (4) | 88.23 | Very Good |
| (5) | 83.71 | Good |
| (6) | 90.24 | Very Good |
| (7) | 92.43 | Very Good |
| (8) | 8.73 | Very Good |
| (9) | 89.64 | Very Good |
| (10) | 86.51 | Very Good |

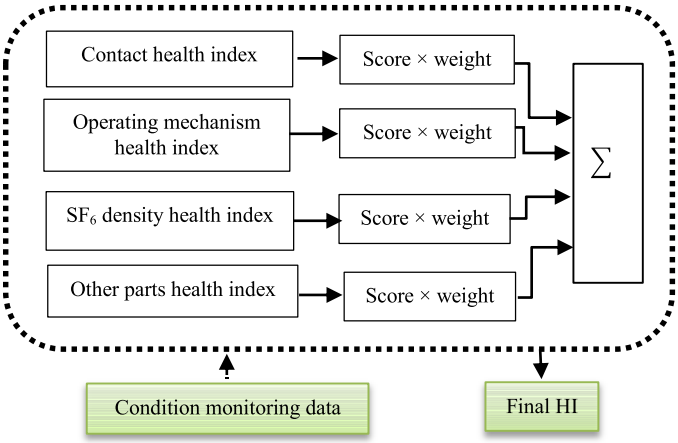



Fig. 9. Diagnosis system architecture.

The contact condition assessment module described in this paper is a part of an overall diagnosis architecture based on HI. Fig. 9 shows the proposed architecture of this system. Combination of each module HI will provide an enhanced insight into the condition of a CB.

## VI. CONCLUSION

The method to assess the condition of electrical contacts is proposed using five criteria as $R_a$ (m$\Omega$), $R_p$ (m$\Omega$), $R_a \cdot T_a$ (m$\Omega \cdot$ ms), $T_{\text{ov}}$ (ms), and $R_{a,\max}$ (m$\Omega$) extracted from dynamic resistance waveform. For each criterion, using scoring and weighting techniques, HI is applied to classify the input data to levels of severity: healthy, moderate, and risk. The details of scoring and assigned weighting of each criterion are presented in this paper. Knowing the HI, corrective or major maintenance (for very poor and poor operation), PM (for fair and good state), as well as no maintenance action (for healthy state) can be reasonably planned. To evaluate the efficiency of the proposed method, ten healthy and ten deteriorated electrical contacts are chosen. The results show the condition of electrical contacts will be accurately determined using this approach. Thus, HI can be employed to provide significant information about the overall condition of electrical contacts.

Authorized licensed use limited to: Electricity Generating Authority of Thailand. Downloaded on January 15,2021 at 00:33:40 UTC from IEEE Xplore. Restrictions apply.

## REFERENCES


[1] S. S. Biswas, A. K. Srivastava, and D. Whitehead, "A real-time data-driven algorithm for health diagnosis and prognosis of a circuit breaker trip assembly," *IEEE Trans. Ind. Electron.*, vol. 62, no. 6, pp. 3822–3831, Jun. 2015.

[2] S. E. Rudd, V. M. Catterson, S. D. J. McArthur, and C. Johnstone, "Circuit breaker prognostics using $SF_6$ data," in *Proc. IEEE Power Soc. General Meeting*, San Diego, CA, USA, Jul. 2011, pp. 1–6.

[3] J. Swingler, A. Sumption, and J. W. McBride, "The evolution of contact erosion during an opening operation at 42 V," in *Proc. 51st IEEE Holm Conf. Elect. Contacts*, Sep. 2005, pp. 346–351.

[4] M. Landry, O. Turcotte, and F. Brikci, "A complete strategy for conducting dynamic contact resistance measurements on HV circuit breakers," *IEEE Trans. Power Del.*, vol. 23, no. 2, pp. 710–716, Apr. 2008.

[5] R. T. de Souza and E. G. da Costa, "Analysis of the correlation between the level of contact degradation and the dynamic resistance curve in circuit breakers," *J. Energy Power Eng.*, vol. 8, pp. 1104–1111, Jun. 2014.

[6] M. Landry *et al.*, "A new measurement method of the dynamic contact resistance of HV circuit breakers," in *Proc. IEEE PES Transmiss. Distrib. Conf. Exhibit.*, May 2006, pp. 1002–1009.

[7] J. Tepper, M. Seeger, T. Votteler, V. Behrens, and T. Honig, "Investigation on erosion of Cu/W contacts in high-voltage circuit breakers," *IEEE Trans. Compon. Packag. Technol.*, vol. 29, no. 3, pp. 658–665, Sep. 2006.

[8] CIGRE Working Group 13.06, "Final report of the second international enquiry on high voltage circuit breaker failures and defects in service," Paris, France, Aug./Sep. 1994.

[9] C. R. Heising, "Worldwide reliability survey of high-voltage circuit breakers," *IEEE Ind. Appl. Mag.*, vol. 2, no. 3, pp. 65–66, May/Jun. 1996.

[10] A. Šečić and B. Milovic. *Dynamic Resistance Measurement Method Applying High DC Current*, accessed on Jan. 16, 2016. [Online]. Available: http://www.amforum.org/site/journal/breakers%20drm.pdf

[11] F. Salamanca, F. Borras, H. Eggert, and W. Steingrber, "Preventive diagnosis on high voltage circuit breaker," in *Proc. CIGRE Symp.*, Berlin, Germany, 1993, pp. 120-02.

[12] R. K. Tyagi and N. S. Sodha, "Condition-based maintenance techniques for EHV-class circuit breaker," presented at the Doble Client Conf., Boston, MA, 2001.

[13] M. Ohlen, B. Dueck, and H. Wernli, "Dynamic resistance measurements—A tool for circuit breaker diagnostics," in *Proc. Power Tech. Int. Symp. Electr. Power Eng.*, vol. 6. Stockholm, Sweden, 1995, pp. 108–113.

[14] R. T. de Souza, E. G. da Costa, J. F. de Araújo, and E. C. T. de Macêdo, "A system for dynamic contact resistance with Arduino platform on MV and HV circuit breaker," in *Proc. IEEE Int. Instrum. Meas. Technol. Conf. (I2MTC)*, Montevideo, Uruguay, May 2014, pp. 369–373.

[15] K. Obarčanin, A. Šečić, and N. Hadžimejlić, "Design and development of the software solution for analysis and acquisition of the high voltage circuit breakers dynamic resistance measurement results," in *Proc. 38th Int. Conv. Inf. Commun. Technol., Electron. Microelectron.*, Opatija, Croatia, May 2015, pp. 1032–1036.

[16] R. T. de Souza, E. G. da Costa, A. C. de Oliveira, W. de V. Sousa, and T. C. M. de Morais, "Characterization of contacts degradation in circuit breakers through the dynamic contact resistance," in *Proc. IEEE PES Transmiss. Distrib. Conf. Expo.*, Medellín, Colombia, Sep. 2014, pp. 1–6.

[17] P. Gill, *Electrical Power Equipment Maintenance and Testing*. Boca Raton, FL, USA: CRC Press, 2008.

[18] *Dynamic Resistance Measurement: Part of the Analysis Inspection Service*, accessed on Apr. 14, 2015. [Online]. Available: http://www.abb.com/

[19] T. Suwanasri, C. Suwanasri, S. Nobnorp, and S. Wattanawongpitak, "Performance evaluation based on symptom, failed-type and obsolescence criteria of high voltage circuit breaker," in *Proc. 10th Int. Conf. Elect. Eng./Electron., Comput., Telecommun. Inf. Technol. (ECTI-CON)*, May 2013, pp. 1–4.

[20] P.-C. Lin, J.-C. Gu, and M.-T. Yang, "Intelligent maintenance model for condition assessment of circuit breakers using fuzzy set theory and evidential reasoning," *IET Generat., Transmiss. Distrib.*, vol. 8, no. 7, pp. 1244–1253, Jul. 2014.

[21] C. Kobashikawa, Y. Hatakeyama, F. Dong, and K. Hirota, "Fuzzy algorithm for group decision making with participants having finite discriminating abilities," *IEEE Trans. Syst., Man, Cybern. A, Syst., Humans*, vol. 39, no. 1, pp. 86–95, Jan. 2009.

[22] W.-H. Chen, "Quantitative decision-making model for distribution system restoration," *IEEE Trans. Power Syst.*, vol. 25, no. 1, pp. 313–321, Feb. 2010.

[23] V.-N. Huynh, Y. Nakamori, T.-B. Ho, and T. Murai, "Multiple-attribute decision making under uncertainty: The evidential reasoning approach revisited," *IEEE Trans. Syst., Man, Cybern. A, Syst., Humans*, vol. 36, no. 4, pp. 804–822, Jul. 2006.

[24] J. C. Helton, "Uncertainty and sensitivity analysis techniques for use in performance assessment for radioactive waste disposal," *Rel. Eng. Syst. Safety*, vol. 42, nos. 2–3, pp. 327–367, 1993.

[25] M. E. Ricotti and E. Zio, "Neural network approach to sensitivity and uncertainty analysis," *Rel. Eng. Syst. Safety*, vol. 64, no. 1, pp. 59–71, 1999.

[26] D. S. Yeung, I. Cloete, D. Shi, and W. W. Y. Yng, *Sensitivity Analysis for Neural Networks*. Heidelberg, Germany: Springer, 2009.

[27] A. A. Bhole and W. Z. Gandhare, "An overview of dynamic contact resistance measurement of HV circuit breakers," *J. Inst. Eng. (India) B*, vol. 97, no. 2, pp. 219–226, Jan. 2015.

[28] N. S. Sodha, S. Singh, S. Victor, and R. K. Tyagi, "Condition assessment of EHV class circuit breakers using dynamic contact resistance measurement technique," in *Proc. CIGRE Session*, Paris, France, 2012, pp. 1–11.

[29] A. N. Jahromi, R. Piercy, S. Cress, J. R. R. Service, and W. Fan, "An approach to power transformer asset management using health index," *IEEE Elect. Insul. Mag.*, vol. 25, no. 2, pp. 20–34, Mar./Apr. 2009.

[30] C. Neumann *et al.*, "Strategy for end of life assessment for high voltage circuit breakers," in *Proc. CIGRE Session*, France, Paris, 2008, p. A3-101.

[31] T. Hjartarson and S. Otal, "Predicting future asset condition based on current health index and maintenance level," in *Proc. IEEE 11th Int. Conf. Transmiss. Distrib. Construction, Oper. Live-Line Maintenance*, Oct. 2006, pp. 1–8.

[32] R. D. Garzon, *High Voltage Circuit Breakers: Design and Applications*, 2nd ed. New York, NY, USA: Marcel Dekker, 2002.




**Maryam Khoddam** was born in Arak, Iran, in 1985. She received the B.Sc. degree in electrical engineering from Bu-Ali Sina University, Hamedan, Iran, in 2007, and the M.Sc. degree in electrical engineering from Shahid Beheshti University, Tehran, Iran, in 2011. She is currently pursuing the Ph.D. degree with the Ferdowsi University of Mashhad, Mashhad, Iran.

Her current research interests include monitoring of power components and power system protection.



**Javad Sadeh** was born in Mashhad, Iran, in 1968. He received the B.Sc. and M.Sc. degrees (Hons.) from the Ferdowsi University of Mashhad, Mashhad, in 1990 and 1994, respectively, and the Ph.D. degree from the Sharif University of Technology, Tehran, Iran, in collaboration with the Electrical Engineering Laboratory, Institute National Polytechnique de Grenoble, Grenoble, France, in 2001, all in electrical engineering.

He is currently a Professor with the Department of Electrical Engineering, Ferdowsi University of Mashhad, and the Deputy Dean for education and postgraduate studies. His research interests include power system monitoring, protection, dynamics, and operation.



**Pedjman Pourmohamadiyan** was born in Tehran, Iran, in 1976. He received the B.Sc. degree from Shiraz University, Shiraz, Iran, in 1998, and the M.Sc. and Ph.D. degrees from the University of Tehran, in 2001 and 2010, respectively, all in electrical power engineering.

He was an Assistant Professor with the Ferdowsi University of Mashhad, Mashhad, Iran, from 2011 to 2014. He is currently the Manager of HVdc Valve Electrical Design with ABB, Ludvika, Sweden. His current research interests include HV apparatus failure diagnosis, gas discharge, and circuit breakers.

Authorized licensed use limited to: Electricity Generating Authority of Thailand. Downloaded on January 15,2021 at 00:33:40 UTC from IEEE Xplore. Restrictions apply.